IV MITIGATION OF EARTHQUAKE AND LIQUEFACTION EFFECTS

EXPERIMENTS ON FORCE ACTING ON UNDERGROUND STRUCTURES IN LIQUEFACTION-INDUCED GROUND FLOW

Masakatsu MIYAJIMA[1] and Masaru KITAURA[2]

ABSTRACT

The present paper focuses on the effects of force induced by liquefied ground flow on underground structures. Small scale tests were conducted using model sand deposits in order to understand the characteristics of liquefied soil. According to the tests, the soil layers showed performance like a liquid when the excess pore water pressure ratio was equal to 1.0, that is, complete liquefaction. Next, the viscous coefficient of completely liquefied soil was estimated from the test that was called dropping ball method As a result, the viscous coefficient of completely liquefied sand was about 10^5 times greater than that of water Moreover, bending strains of a model pile in liquefied ground flow were measured and compared with those calculated by using the viscous coefficients obtained from the previous experiments. It is concluded that the viscous coefficient obtained from the dropping ball method could be applied to estimation of the force acting on underground structures in liquefied ground flow.

1) Associate Professor, Dept. of Civil Engineering, Kanazawa University, 2-40-20 Kodatsuno, Kanazawa 920 JAPAN.
2) Professor, ditto

INTRODUCTION

Permanent ground displacement induced by soil liquefaction is one of the most serious liquefaction hazards. Many civil engineering structures, especially lifeline facilities have been damaged by the liquefaction-induced permanent ground displacement Hamada and O'Rourke investigated liquefaction-induced permanent ground deformation and lifeline performance during past earthquakes in Japan and U.S.A. from the 1906 San Francisco earthquake to the 1989 Loma Prieta earthquake through the Japan-U.S. cooperative research program [1]. Many studies have been performed in order to clarify the mechanisms of generation of liquefied ground flow and to estimate the value of permanent ground displacement [2-5].

A soil spring constant is usually used for the evaluation of seismic response of underground structures so far. Therefore, some liquefaction-related experiments dealing with the soil spring constant have been conducted [6-8]. They concluded that the soil spring constant of liquefied ground became less than 1/10 to 1/1000 of that in the non-liquefied ground It is, however, considered that the behavior of soil deposits with so small spring constant is close to liquid rather than solid. From the point of view, some studies dealing with liquefied ground flow as viscous flow were conducted [9-12]. Takada et al. and Ohtomo et al. concluded that the viscous coefficient of completely liquefied sand layer was about 10^5 times greater than that of water [9,12].

In the present paper, effects of degree of liquefaction on characteristics of soil deposit were clarified. Then, the viscous coefficient of completely liquefied soil was investigated through the small scale tests, so called dropping ball method. Furthermore, vibration tests using a model pile were conducted and the performance of the model pile in liquefied ground flow was measured. The response of the pile was compared with that calculated by using the viscous coefficients obtained from the previous tests

EFFECTS OF DEGREE OF LIQUEFACTION ON CHARACTERISTICS OF SOIL DEPOSITS

A general view of test apparatus is shown in Fig 1 The sand box was 220 mm in width, 380 mm in length and 250 mm in height. River sand was used in the experiments Table 1 lists its material properties Water flow was generated from the bottom of sand deposits and the excess pore water pressure ratio in the sand deposits was controlled by the discharge of water. A ball on two rails was pulled by a motor horizontally. The force was measured by a load cell shown in Fig. 1 when the motor pulled the ball. The displacement of the ball was also measured.

Fig. 2 indicates one of the results obtained here. This figure shows the relationship between the load and displacement of the ball. Five curves in this figure shows the results in case of the excess pore water pressure ratios of 0.00, 0.25, 0.50, 0.75, 1.00, respectively. The velocity of the ball was 1.1 cm/s in this case The load increased at first, then kept a constant value.

Fig. 3 illustrates the maximum load in relation to the pulling velocity and excess pore water pressure ratio. The maximum load decreased with an increase in the excess pore water pressure ratio In case of the excess pore water ratio of less than 1.0, the maximum load decreased with an increase in the pulling velocity Since the load depends on the pulling velocity in case of the excess pore water pressure ratio of less than 1.0, the effects should be considered in evaluation of force acting underground structures While the load increased with an increase in the pulling velocity when the excess pore water pressure was 1.0, so called complete liquefaction. This means that the soil layers showed the behavior of viscous fluid when the excess pore water pressure ratio was equal to 1.0 The present paper focuses on the force induced by completely liquefied ground because the soil layers with a slope deformed after complete liquefaction.

VISCOSITY OF COMPLETELY LIQUEFIED SOIL

Viscous coefficients of completely liquefied soil were measured in order to evaluate the force acting on underground structures in liquefied ground flow. The general view of test apparatus was shown in Fig 4. The sand container was plastic cylinder with 380 mm in diameter and 500 mm in height. The sand used in the tests was the same as that in the previous tests The sand container was vibrated by a sinusoidal wave with 5 Hz in frequency. When the sand layer completely liquefied, the ball began to fall into the liquefied sand layer At this stage, the viscous coefficients of the liquefied soil layer can be evaluated from the equilibrium of viscosity resistance, weight of the ball and buoyancy acting on the ball. Two balls were used in the tests. One was 7.8 cm in diameter and 1,160 gf in weight. The other was 3.6 cm in diameter and 150 gf in weight, respectively. The excess pore water pressures and displacement of the ball were measured at each point shown in Fig. 4.

The viscous coefficient was calculated using the following equations. A completely liquefied ground was assumed as the Newtonian fluid in this study. According to the Stokes' formula, the viscosity resistance acting on a ball in the Newtonian fluid can be expressed as Eq (1) when the ball with diameter a fell in viscous fluid at a steady speed of V [13].

$$F = 6\pi a \mu V \tag{1}$$

Here F is resistance acting on a ball , a is diameter of the ball, μ is viscous coefficient and V is relative velocity between the ball and surrounding soil The equilibrium equation of viscosity resistance, weight of ball and buoyancy acting on the ball when the ball is falling at a steady speed in the viscous fluid is as follows:

$$6\pi a \mu V = 4\pi a^3 (\rho' - \rho) g / 3 \tag{2}$$

Here ρ is density of fluid, ρ' is density of the ball and g is acceleration of gravity The viscous coefficient μ can be obtained from the following equation

$$\mu = \frac{4\pi a^2 (\rho' - \rho) g}{18\pi V} \tag{3}$$

Fig 5 illustrates one of the test results The time histories of response acceleration of the sand container, displacement of the ball and excess pore water pressure ratios are indicated, respectively. These figures indicate that the ball began to fall when the excess pore water pressure ratio reached 1.0, then the ball was falling in the liquefied soil layer at a steady speed for more than 5 seconds

Fig 6 indicates the viscous coefficient calculated from Eq (3) in relation to the input acceleration. According to this figure, the viscous coefficient obtained here was not correlated with the input acceleration and ball diameter despite a somewhat scatter in individual data points The data points distribute from 0 71 gf s/cm^2 to 3 22 gf s/cm^2, and the average in this figure is 1 67 gf s/cm^2

RESPONSE OF MODEL PILE IN LIQUEFIED GROUND FLOW

Model Test

The diagram of the experimental apparatus is shown in Fig 7. The sand box was 500 mm in width, 1500 mm in length and 350 mm in height. The model sand deposits had a slope of 6 % to 10 %. The sand deposit was made from loose saturated sand, whose material properties were the same as those listed in Table 1. The model pile was simulated by a rubber rod with 10 mm in diameter and 130 mm in length. Its elastic modulus was 810 kgf/cm^2 and its weight per unit volume was 1.14 gf/cm^3 as listed in Table 2. Two strain gauges were utilized at the model pile. Twenty-four pins were installed at the surface of the sand stratum to measure horizontal residual displacements of the ground surface. The deformation of the ground surface during excitation was measured by means of a video camera. The model sand stratum was vibrated by a harmonic wave with 5 Hz. Input acceleration of the table was 150 cm/s^2.

Fig. 8 illustrates the average velocity of the pins shown in Fig. 7. The pins did not move till the excess pore water pressure ratio reached 1.0. Therefore, the average velocities after completely liquefaction were shown in Fig. 8. The average velocity was evaluated from the displacement for 2 seconds at every time step. This figure indicates the duration time of ground deformation for 6 % slope is shorter than that for 10 % slope despite that the duration time of complete liquefaction was almost same This could be considered as follows The upper portion of soil deposit subsided and the lower potion heaved up when the liquefaction of sand layer occurred. The slope of soil deposit became gentle and finally horizontal. Therefore, it is conceivable that the larger the slope of soil deposit is, the longer the duration of ground deformation is. The average velocities of the pins, that is, velocity of ground deformation, were 1.6 cm/s for 10% slope and 0.9 cm/s for 6% slope, respectively. It suggests the velocity of ground deformation increases with an increase in slope of ground This result is similar to other test results conducted by Miyajima et al. [14].

Discussion

Now, a vertical distribution of velocity is considered here when a viscous fluid flows on an inclined plate under the condition of stationary, shown in Fig 9. The equation governing the motion of a viscous fluid is given as follows:

$$\mu \frac{\partial^2 V_g}{\partial x^2} + \rho g \cos\beta = 0 \tag{4}$$

in which V_g is velocity of a fluid, ρ is density of the fluid, μ is viscous coefficient, β is slope of the inclined plane and δ is thickness of the fluid, respectively. The boundary conditions are

$$x = 0 : \frac{dV_g}{dx} = 0 \tag{5}$$

$$x = \delta \cdot V_g = 0 \tag{6}$$

By integrating Eq. (4) with respect to x using the boundary conditions Eqs (5) and (6), the analytical solution is obtained as follows:

$$V_g(x) = \frac{\rho g \delta^2 \cos\beta}{2\mu} \left\{ 1 - \left(\frac{x}{\delta} \right)^2 \right\} \tag{7}$$

Fig. 10 shows the vertical distribution of velocity calculated by using Eq. (7). The viscous coefficient of 1.67 gf s/cm^2 was used in this case This value was obtained from the tests in the previous chapter. According to this figure, the maximum velocities of liquefied sand deposit at the surface were 10.07 cm/s for 10% slope and 8.07 cm/s for 6% slope, respectively. These values are larger than those obtained from the model tests. The velocity is evaluated as larger value if the viscous coefficient obtained from the tests is used The equation governing the motion of the fluid is constructed under the condition of stationary, however the model tests were not stationary state. It is conceivable that this could cause the difference of the values. The effect of the wall of sand box was also considered as one of reasons

The liquefied ground flow is assumed as the viscous fluid on inclined plate here The bending moment of the model pile was calculated using the distribution of velocity shown in Fig. 10. The force acting on the pile in the liquefied ground flow was evaluated as follows.

$$f = \rho C_d V_r^2 D / 2 \tag{8}$$

Here f is the force, ρ is density of liquefied ground, C_d is resistance factor, V_r is relative velocity between the model pile and liquefied ground flow and D is diameter of the model pile. The resistance factor for a cylinder in the fluid with low Reynolds' number can be expressed as:

$$C_d = 8\pi / R_e \{0.5 - \alpha - \ln(R_e / 8)\} \tag{9}$$

in which R_e is Reynolds' number and α is Euler's constant. Reynolds' number can be given as:

$$R_e = V_r D / \nu \tag{10}$$

Here ν is kinematic viscosity The relation between viscous coefficient and kinematic viscosity can be expressed as follows

$$\mu = \nu \rho \tag{11}$$

Fig. 11 illustrates the bending moment of the model pile calculated by using equations above mentioned. the dots in this figure show the bending moment calculated from the bending strains measured in the tests. The values calculated show good agreement with the measured values It suggests that the viscous coefficient obtained from the dropping ball method can be used for estimation of the force acting on underground structures in liquefied ground flow.

CONCLUDING REMARKS

The effects of force acting on underground structures in liquefied ground flow were investigated in the present paper. The sand soil layers behaved as a viscous fluid after the excess pore water pressure ratio reached 1.0, that is, after complete liquefaction Therefore, the completely liquefied soil was treated as a viscous liquid. Small scale test were conducted in order to measure the viscous coefficient of liquefied sand. The dropping ball method gave the viscous coefficient of 1 67 gf s/cm^2. The viscous coefficient obtained here were about 10^5 times greater than that of water

Furthermore, vibration tests using a model pile were conducted and the response of the model pile in liquefied ground flow was measured. The response of the pile was compared with that calculated by using the viscous coefficients obtained from the previous tests. As a result, the viscous coefficient obtained from the small scale tests can be used for estimation of the force acting on underground structures in liquefied ground flow.

ACKNOWLEDGEMENTS

The authors wish to thank Mr. Masamichi Hasegawa (graduate student of Kanazawa University) and Mr. Hidemasa Hosaka (student of Kanazawa University) for their cooperation in experiments. A part of expense of this study was defrayed by Kawasaki Steel Corporation.

REFERENCES

1) Hamada, M and O'Rourke T.D. (Edit.) Case Studies of Liquefaction and Lifeline Performance During Past Earthquake, Vols 1 and 2, Technical Report NCEER-92-0001, 0002, 1992.
2) Hamada, M., Yasuda, S., Isoyama, R. and Emoto, K : Study on Liquefaction-Induced Permanent Ground Displacements and Earthquake Damage, Proceedings of JSCE, No. 376, pp. 221-229, 1986 (in Japanese).
3) Towhata, I., Finite Element Model to Predict Permanent Displacement of Ground Induced by Liquefaction, Proc. 2nd Int Conf Numer Meth Geomech., pp. 689-697, 1986.
4) Miyajima, M., Kitaura, M. and Nomura, Y.: Study on Response of Buried Pipelines Subjected to Liquefaction-induced Permanent Ground Displacement, Proceedings of JSCE, No. 404, pp 163-172, 1989.
5) Yasuda, S., Nagase, H., Kiku, H. and Uchida, Y.: The Mechanism and a Simplified Procedure for the Analysis of Permanent Ground Displacement Due to Liquefaction, Soils and Foundations Proceedings of JSSMFE, Vol. 32, No. 1, pp. 149-160, 1992
6) Yasuda, S., Saito, K and Suzuki, N : Soil Spring Constant on Pipe in Liquefied Ground, Proceedings of the 19th JSCE Earthquake Engineering Symposium, pp 189-192, 1987 (in Japanese).
7) Tanabe, K.: Fundamental Study on Seismic Assessment and Design of Buried Pipeline Subjected to Ground Failure During Earthquake, Doctoral Dissertation Submitted to Kobe University, Chapter 5, 1988 (in Japanese).
8) Miyajima, M and Kitaura, M.: Experiments on Soil Spring Constants During Liquefaction, Proceedings of the 2nd Intl. Conf. on Recent Advances in Geotechnical Earthquake Engineering and Soil Dynamics, Vol. 1, pp 487-490, 1991
9) Takada, S. and Nagai, J.: Dynamic Stiffness and Damping in Liquefied Ground, Construction Engineering Laboratory Report, No. 29, pp. 53-72, 1987 (in Japanese).
10) Sato, H., Doi, M, Hamada, M. and Nakamura, T.: Analysis of Liquefied Ground Flow and Its Consideration, Proceedings of the 22nd JSCE Earthquake Engineering Symposium, pp. 87-90, 1993 (in Japanese)
11) Doi, M., Sato, H. and Hamada, M Experimental Study on Behavior of Liquefied Ground Flow and Its Characteristics, Proceedings of the 22nd JSCE Earthquake Engineering Symposium, pp 91-94, 1993 (in Japanese)
12) Ohtomo, K., Iwatate T., Shimizu, M., Shumuta, Y and Hamada, M.: Characteristics of Load Acting on Pile Foundation in Liquefied Ground Flow, Proceedings of the 22nd JSCE Earthquake Engineering Symposium, pp 95-98, 1993 (in Japanese).
13) Graf, W. H.: Hydraulics of Sediment Transport, McGraw-Hill Book Co., N.Y., 1971.
14) Miyajima, M., Kitaura, M. and Ando, K : Experimental Study on Permanent Deformation of Liquefied Ground, Proceedings of the 8th Japan Earthquake Engineering Symposium, pp 939-944, 1990 (in Japanese)

Table 1 Physical properties of sand.

Specific Gravity	2.67	
Uniformity Coefficient	2.96	
Maximum Void Ratio	1.030	
Minimum Void Ratio	0.721	
50 Percent Diameter	0.2	(mm)
Coefficient of Permeability	1.92 $\times 10^{-2}$	(cm/s)

Table 2 Physical properties of pile model.

Young's modulus	810	(kgf/cm^2)
Unit weight	1.14	(gf/cm^3)
Length	130	(mm)
Diameter	10	(mm)

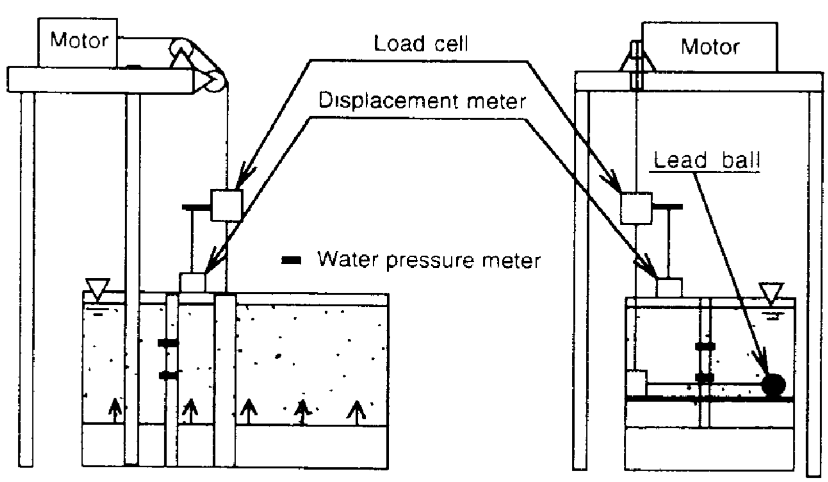

Fig. 1 General view of test apparatus.

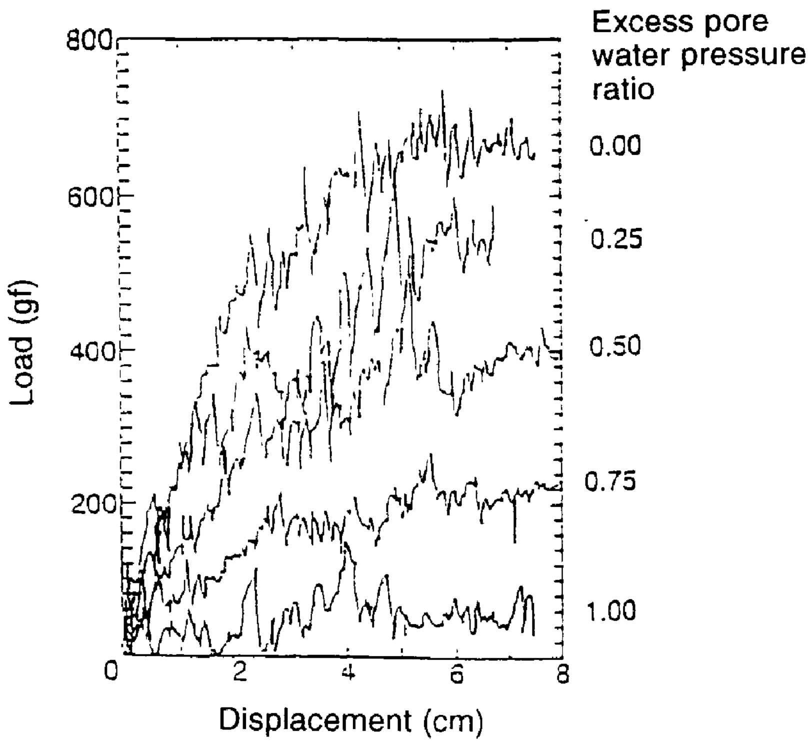

Fig. 2 Relationship between load and displacement.

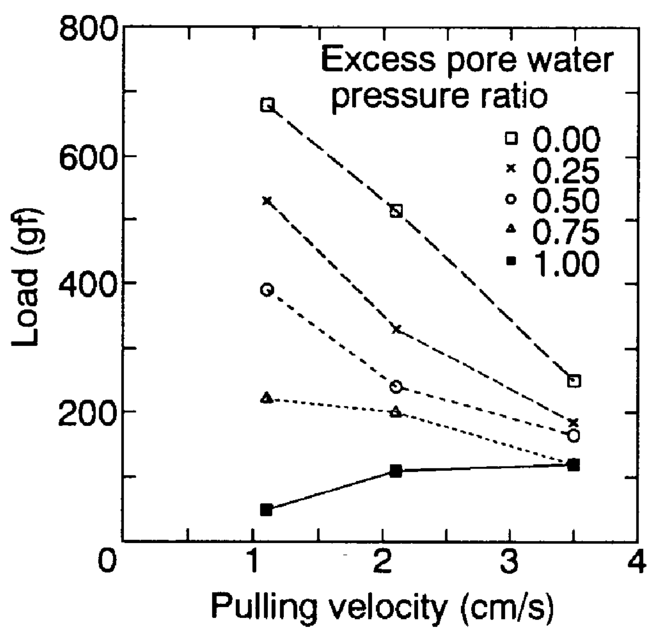

Fig. 3 Relationship between maximum load and pulling velocity.

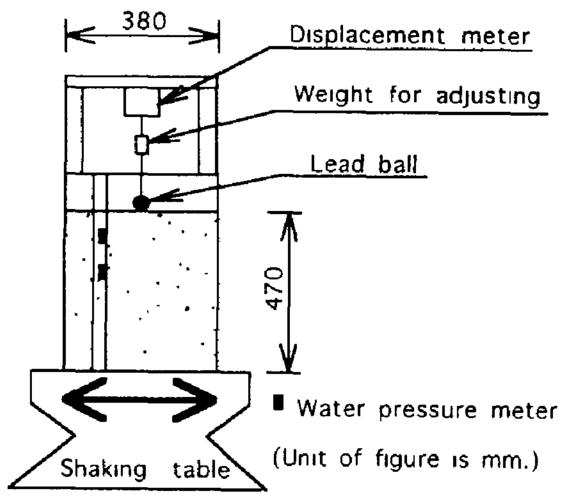

Fig. 4 General view of test apparatus for dropping ball method.

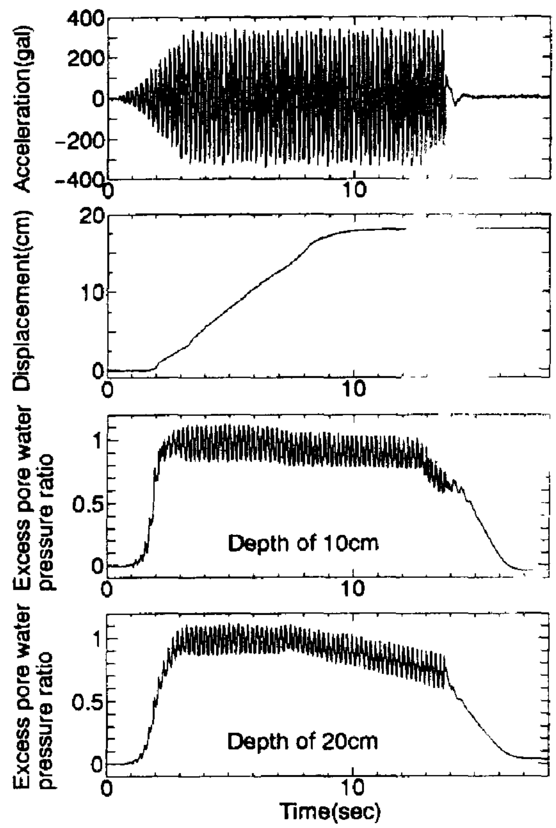

Fig. 5 Time histories of response acceleration, displacement and excess pore water pressure ratios.

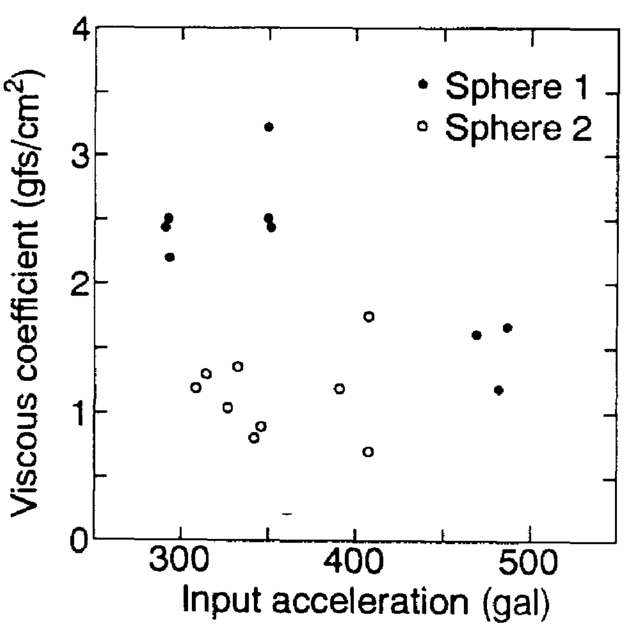

Fig. 6 Relationship between input acceleration and viscous coefficient.

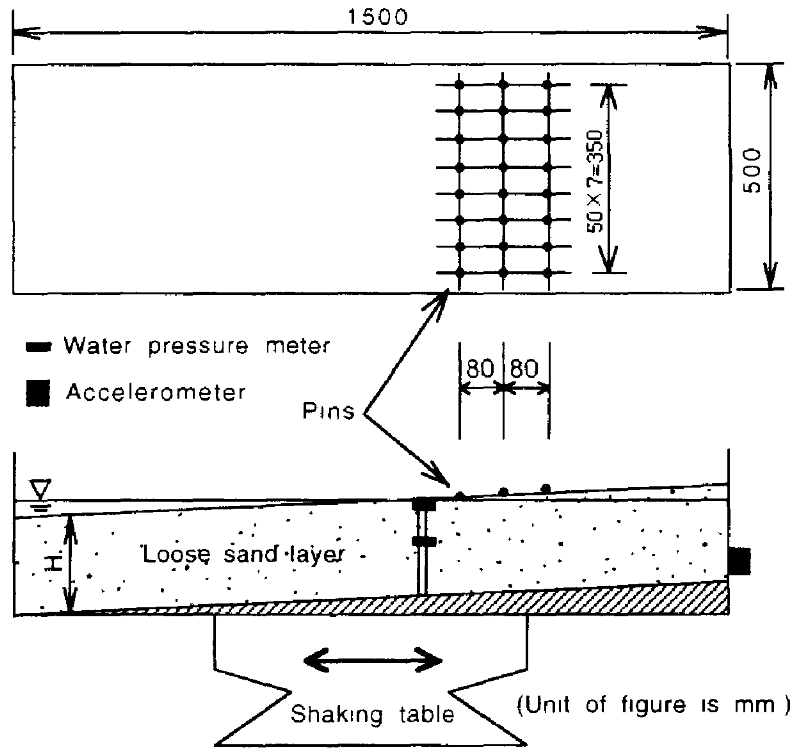

Fig. 7 General view of test apparatus for liquefied ground flow.

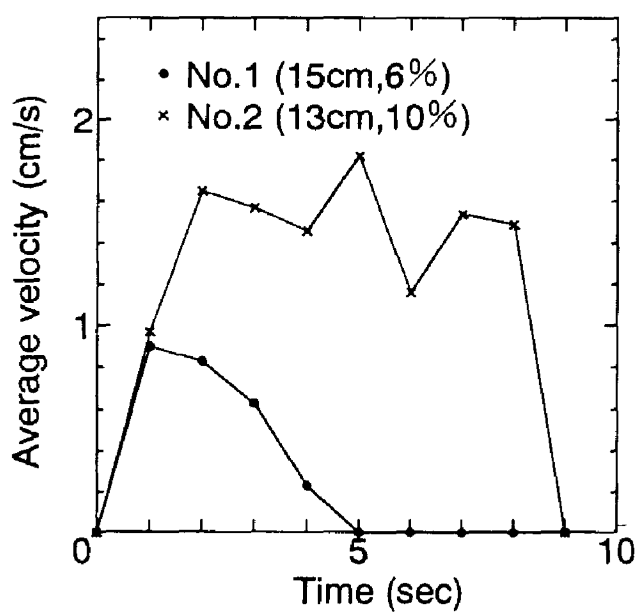

Fig. 8 Velocity of ground deformation at surface.

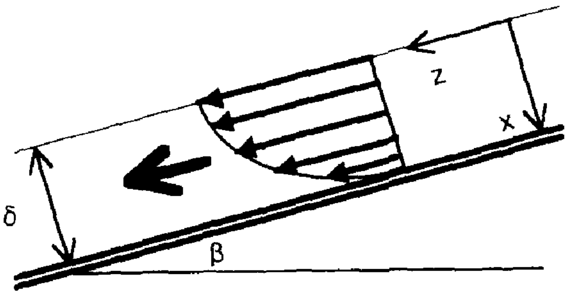

Fig. 9 Model of liquid flow on inclined plate.

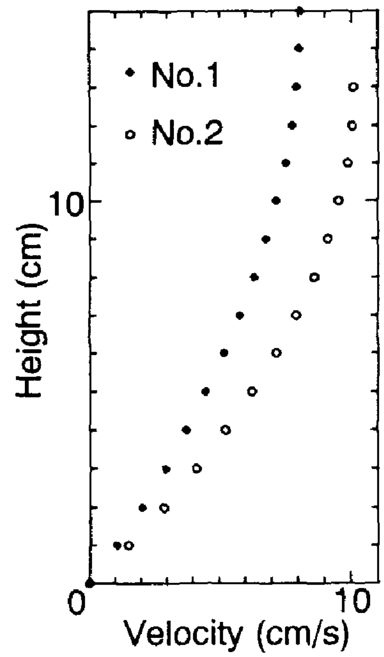

Fig. 10 Theoretical distribution of velocity.

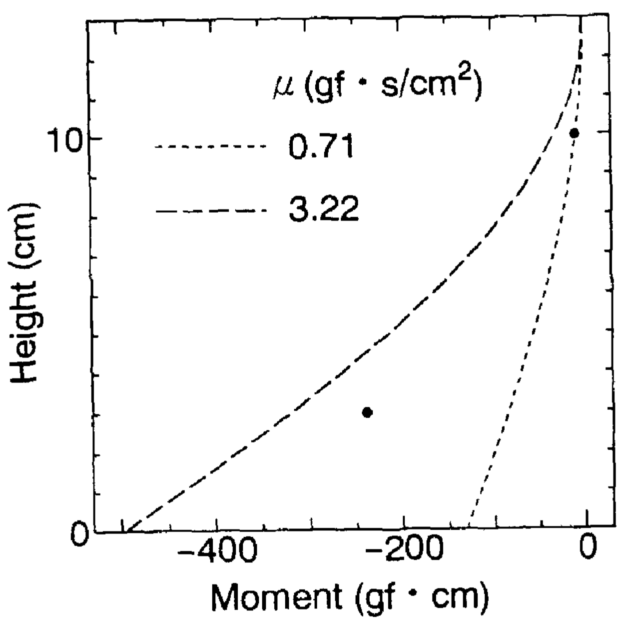

Fig. 11 Relationship between bending moment obtained by model test and analysis.